Available online at www.sciencedirect.com
SCIENCE DIRECT
Polymer 47 (2006) 5003–5011
polymer
www.elsevier.com/locate/polymer

Ex situ hydrolytic degradation of sulfonated polyimide membranes for fuel cells

Gilles Meyer [a], Carine Perrot [a], Gérard Gebel [a,*], Laurent Gonon [a], Sandrine Morlat [b], Jean-Luc Gardette [b]

[a] *Département de Recherche Fondamentale sur la Matière Condensée, SPrAM/Groupe Polymères Conducteurs Ioniques, UMR 5819 (CEA-CNRS-UJF), CEA-Grenoble, 17 rue de Martyrs, 38054 Grenoble cedex 9, France*
[b] *Laboratoire de Photochimie Moléculaire et Macromoléculaire UMR 6505 (CNRS-UBP), Ensemble Universitaire des Cézeaux, 63177 Aubière, France*

Received 22 July 2005; received in revised form 15 November 2005; accepted 11 April 2006
Available online 30 May 2006

Abstract

Ex situ hydrolytic stability of sulfonated polyimide (s-PI) membranes for fuel cells was studied depending on structural and external parameters including the ion exchange capacity, the block character, the temperature and the hydrogen peroxide concentration. Infrared spectroscopy was used to identify and quantify the chemical modifications such as the loss of imide functions and of ionic monomers. The decrease in ion exchange capacity due to the elution of sulfonated oligomers was confirmed by sulfur content analysis. A complete hydrolysis of some of the imide functions is observed leading to polymer chain scissions and to the loss of the mechanical properties. It is shown to be a thermo activated process and the activation energy (60 kJ/mol) is found in good agreement with the value determined from fuel cell lifetimes. The degradation in fuel cell conditions is similar but faster than in pure water. The same kinetic can be reproduced ex situ by addition 0.05% of hydrogen peroxide.

Keywords: Fuel cells; Proton conducting membranes; Sulfonated polyimides

1. Introduction

Proton exchange membrane fuel cells (PEMFC) are considered as the most promising power source for automotive and portable applications [1]. The PEMFC core component is the membrane-electrode assembly (MEA) usually based on perfluorosulfonated ionomer membranes (Nafion® type). However, the development of PEMFC prototypes has pointed out some major drawbacks of the perfluorosulfonated materials such as the MEA degradation under cycling conditions, the loss of performance at elevated temperatures and excessive production costs. Alternative low cost membranes with improved properties are thus needed to be developed and many different structures were investigated during the last ten years [2–4]. These structures are mainly sulfonated aromatic thermostable polymers such as polyetherketones, polysulfones, polyparaphenylenes or polybenzimidazoles. Among these new polymers, sulfonated polyimides (sPI) based on naphtahalenic moieties are considered as promising materials owing to their interesting swelling, mechanical and conducting properties [5–10].

Sulfonated polyaromatic membranes exhibit a low stability in fuel cell conditions, which does not exceed 1000 h of operation even under stationary conditions [11]. Up to now, no PEMFC stack with such membranes has been disclosed mainly because of their lack of long-term stability. Surprisingly, the stability is not one of the studied properties for new polymers. Therefore, only few data have been published and adapted quantitative protocols have not been yet developed to evaluate the stability neither in situ in fuel cells nor ex situ. In the literature, most of the works on membrane stability deals with either sulfonated polystyrenes or sulfonated polyimides [12–16]. While polymer chain scissions due to radical attacks have been evidenced for sulfonated polystyrene membranes, the sPI degradation is attributed to a high sensitivity to hydrolysis. Their lifetime under operating conditions was shown to vary from only few tenths of hours to 1000 h depending on the membrane ion exchange capacity (IEC) and the operating temperature [16]. Sulfonated polyimides are synthesized by polycondensation using a commercial naphthalenic dianhydride

* Corresponding author. Tel.: +33 438 783 046; fax: +33 438 785 097.
E-mail address: ggebel@cea.fr (G. Gebel).

0032-3861/$ - see front matter © 2006 Published by Elsevier Ltd.
doi:10.1016/j.polymer.2006.04.007

monomer and different sulfonated and non-sulfonated diamines, which proportions are adjusted to control the IEC value. The main development in the field of sulfonated polyimide membranes is currently the use of chemically modified diamines to enhance the stability against hydrolytic and oxidative attacks [17,18]. The membrane stability is usually estimated through the loss of the mechanical properties when immersed at elevated temperature (80 °C) in either pure water or more or less concentrated hydrogen peroxide solutions (Fenton reactants). However, the evaluation of the loss of mechanical properties is restricted to the determination of the immersion time until membrane dissolution or breaking when lightly bent [19,20]. This measurement is somewhat approximate since there is no information about the degradation kinetics and it strongly depends on the operator. Moreover, the membrane rupture occurs at a critical polymer chain length, which depends on both the initial molecular weight and the polymer chain scission kinetic. Since, molecular weights are not measured independently, an anticipated breaking of the membrane could be attributed a lack of stability while it can be due to a problem encountered during the synthesis, which has limited the polymer chain length.

The main objective of the present work is to characterize the hydrolysis phenomenon by ex situ degradation studies depending on the relevant parameters such as IEC, temperature and block character. The second objective is the development and the validation of new protocols to evaluate quickly the membrane stability instead of performing long and expensive fuel cell tests. These protocols involve infrared spectroscopy (IR), sulfur content determination through the use of energy dispersive X-ray analysis by scanning electron microscopy (SEM EDX) and mechanical properties determination. Finally, the kinetics of ex situ degradation in hydrogen peroxide solutions are compared to the degradation in fuel cell conditions and the appropriate concentration is determined.

2. Experimental

2.1. Materials

Different series of sPI have been synthesized in *m*-cresol by the LMOPS (CNRS, Vernaison, France) based on naphthalenic dianhydride, di amino biphenyl disulfonic acid (BDSA) and a 1:1 mixture of 4-4′ and 3-4′ oxydianiline (ODA) monomers according to the previously described procedure [21]. The one pot two step polycondensation leads to block copolymers characterized by X and Y the average sequence lengths of the sulfonated and non-sulfonated blocks (Fig. 1). The ion content (IEC) was adjusted by the ratio X/Y during the synthesis. In this work, the ionic block length sequence was varied from $X=3$ to 9. Random copolymers ($X=1$) were not studied since the synthesis cannot be performed using the same procedure. For each ionic block length, three polymers were prepared with different IEC values (0.9, 1.3 and 2 mequiv./g corresponding to $X/Y=20/80$, 30/70 and 50/50, respectively, as molar ratio between sulfonated and non-sulfonated diamines). In the following, the notation for sPI polymers will be as IEC/$X-Y$ sPI.

sPI solutions were filtered (5 μm) at elevated temperature to remove the largest aggregates and so forth to avoid macroscopic defects. This filtration does not modify the ionomer composition since the ion exchange capacity of the final material was found to correspond to the theoretical value. Membranes were then prepared by solution casting on a hot glass plate by the CEA-Le Ripault (France). A thermal treatment at 150 °C was applied to eliminate the solvent and to insure a complete imidization reaction. After solvent evaporation, sPI membranes were washed 4 h in 1:1 water methanol solution to remove the residual *m*-cresol. They were then acidified in a 0.5 M sulphuric acid solution in order to eliminate the triethylammonium ion used to solubilize the sulfonated monomer during the polymer synthesis.

2.2. Membrane characterization

Stress–strain curves were obtained using an Instron 4301 with 3 mm/min as test rate. The membranes were cut using a punch with 4.25 and 0.95 mm as nominal gauge length and width, respectively. These small sample dimensions can be used since the membranes are very thin (40 μm) and it limits the area of samples necessary for the experiments. The membrane mechanical properties are very sensitive to the water content in terms of both Young modulus and elongation at break. The membranes were kept immersed in water during the measurements to insure reproducible experimental

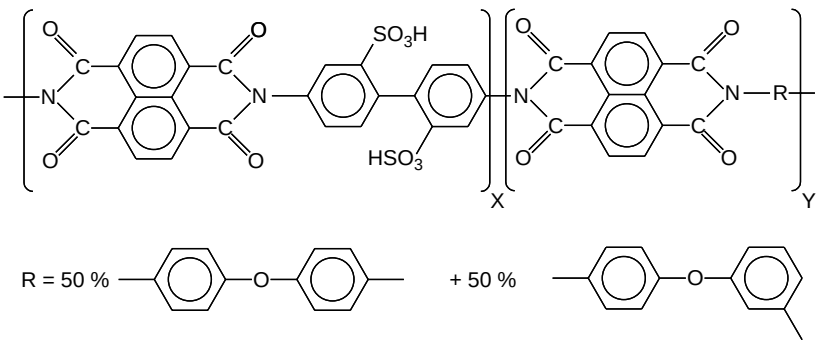

Fig. 1. General chemical formula of sulfonated polyimides.

conditions and because the degraded membranes, which become very brittle are difficult to handle on dry state.

The membrane chemical structure was analyzed by infrared spectroscopy either using an attenuated total reflection (ATR) device with a thunderdome (Ge crystal, penetration depth from 1 to 3 μm depending on the wavelength) directly applied on the membranes or by transmission (Paragon 500 Perkin–Elmer) on thin films (5 μm thick) cast from polymer solutions on ZnSe supports. These solutions were obtained by membrane dissolution in cresol after tetramethyl ammonium neutralization. Thin films were used to avoid too strong infrared absorption and band saturation. The dissolution and casting procedure permits to get average infrared signal either on pristine membrane or on aged materials while ATR technique can be used to study chemical modifications limited to the membrane surfaces.

The sulfur profiles across the membranes were determined by energy dispersive X-ray analysis (EDX) using a Jeol SM840 scanning electron microscope (SEM). Small membrane pieces were imbedded in an epoxy resin prior to observation. A calibration curve was established from the analyses of a series of pristine membranes with ten different IEC values ranging from 0 to 3.5 mequiv./g.

The solid ^{13}C NMR spectra were recorded on a Brucker Avance 400 MHz on crushed samples. Two different NMR sequences were used, CPMAS and HPDEC ('cross-polarization magic angle spinning' and 'high power decoupling'), to visualize by comparison the most mobile carbons. The coupled small-angle and wide angle X-ray scattering experiments (SAXS-WAXS) using simultaneously two detectors have been performed on the ID2 'high brilliance beamline' at the European Synchrotron Radiation Facility (ESRF, Grenoble, France). The incident wavelength was $\lambda = 1$ Å and three sample-to detector distances from 1.5 to 10 m were used to cover the entire SAXS angular range. The samples were neutralized on Cs^+ form prior to experiments in order to increase the contrast between the ionic and hydrophobic phases. The samples were studied either equilibrated at room humidity or equilibrated in liquid water in specific cells with mica windows. The transfer momentum, q, is defined as $q = 4\pi \sin\theta/\lambda$ where θ is the scattering angle. Usual corrections to subtract background and to normalize intensities were applied to the data.

The fuel cell tests were performed on an Electrochem test bench using a 25 cm^2 active area single cell made of impregnated graphite plates with machined flow channels. The ageing experiments were performed at 80 °C under stationary electric loading conditions (0.2 A/cm^2) with pure hydrogen and oxygen and 3 bar absolute gas pressures. The gas inlet flow was 27 cm^3/min for hydrogen and 42 cm^3/min for oxygen corresponding to a stoechiometry of 1.2 and 1.5, respectively. The electrodes were provided by the Sorapec Company (France) with a catalyst loading of 0.1 mg/cm^2 at the anode and 0.2 mg/cm^2 at the cathode. The electrodes were impregnated with a Nafion solution and were not hot pressed on the membrane in order to be able to easily remove it at the end of the ageing tests.

3. Results and discussion

3.1. Mechanical properties

Typical evolution of the stress–strain curves of $X = 5$ sPI membranes immersed in water obtained for different IEC values (0.9, 1.3 and 2 mequiv./g) are presented in Fig. 2(A). The shapes of the curves are characteristic of an elastic behavior for small strains followed by a linear plastic deformation. As previously observed for similar sPI membranes [18], the stress and the elongation at break are, respectively, significantly larger and smaller compared to Nafion®. However, the use of flexible monomers such as ODA in the hydrophobic sequences and the block copolymer nature increases by a factor of 10 the extent of the plastic behavior compared to very rigid sulfonated homopolymers [18]. As a confirmation, the plastic behavior decreases as the IEC increases.

The effect of ageing in water at 70 °C is presented for 2/5-5 sPI in Fig. 2(B). A slight but continuous decrease of both the stress at the flow threshold and of the Young modulus is observed. This can be attributed to plasticization of the polymer by water molecules that can diffuse very slowly in

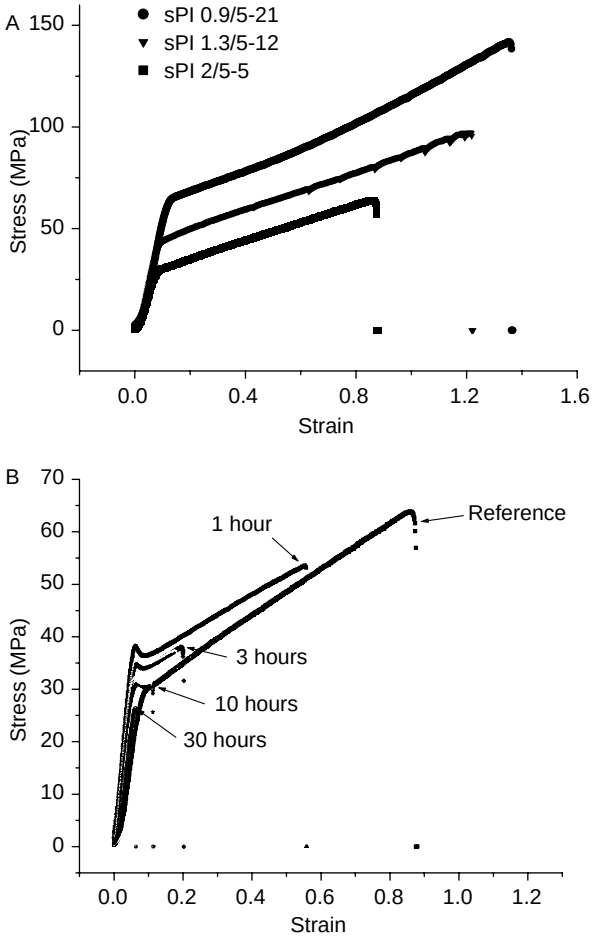

Fig. 2. (A) Stress–strain curves obtained for sPI reference membranes immersed in water. (B) Stress–strain curves obtained for 2/5-5 sPI membrane as a function of ageing time in water at 70 °C.

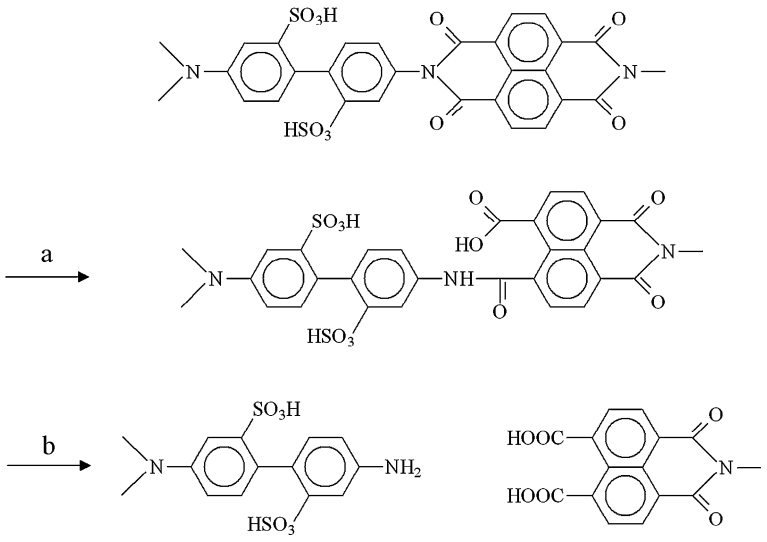

Fig. 3. Hydrolytic reaction of the imide functions.

the non-ionic zones or to a partial hydrolysis of imide functions following the scheme shown in Fig. 3. The complete hydrolysis provokes polymer chain scissions with formation of amine and diacid terminal groups and consequently the loss of the mechanical properties (decrease of the elongation at break). On the contrary, a partial hydrolysis leads to an increase of the polymer chain flexibility without any decrease of the molecular weight. A combination of partial and complete hydrolysis has been already observed for water ageing of model molecules [22]. The difference between the reference and 1 h aged materials is probably attributable to the fact that the pristine membrane has not been immersed in water at high temperature. The main effect of ageing on the mechanical properties is obviously the continuous disappearance of the plastic behavior, which reveals a decrease of the molecular weight consecutive to polymer chain scissions.

The extent of the plastic behavior was determined as a function of ageing time in water at 70 and 90 °C for different IECs. The values normalized with respect to the pristine membrane are plotted in Fig. 4. The elongation at break decreases rapidly for short ageing times. Both temperature and ion content have a drastic effect on the membrane degradation rates as observed in fuel cell conditions [16]. This indicates that hydrolysis is the main degradation process in fuel cells and that the degradation is likely to be mainly localized in the ionic domains. It is worth noting that a non-zero value is observed for the sPI 0.9/5-21 membrane for long ageing times and low degradation temperatures. This behavior suggests that, for low IEC values, the hydrophobic part of the polymer is large enough to maintain some mechanical strength despite the degradation of the ionic sequences. Another possible explanation is that the hydrolysis reaction is equilibrated at low temperature allowing a recombination of the degradation product to form again imide functions. To discriminate between these two possibilities, a study is under progress to verify the appearance of such a plateau for higher IEC values at low ageing temperatures.

3.2. Infrared analysis

The infrared spectra of a pristine 1.3/7-16 sPI membrane and of the same membrane after 1200 h ageing in water at 90 °C are presented in Fig. 5. A series of new IR bands that appears after degradation is clearly visible despite their low intensity (1785, 1600, 1430, 1380 and 1290 cm^{-1}). The 1430 and 1290 cm^{-1} bands are likely to be attributed to carboxylic acid functions (O–H deformation and C–O vibration) while the 1600 cm^{-1} band could corresponds to amine groups (C–N vibration). However, the sPI IR spectra show intense absorption bands, which result from the convolution of several bands in the C=O region [23]. It is, therefore, very difficult to quantitatively analyze this region of the infrared spectrum. The lack of a band corresponding to the C–N deformation at 1510–1570 cm^{-1} that is expected in the case of partial hydrolysis with acid–amide formation suggests that the hydrolysis is primarily a complete reaction (Fig. 3). The 1785 cm^{-1} band can be attributed to the C=O valence vibration of an anhydride.

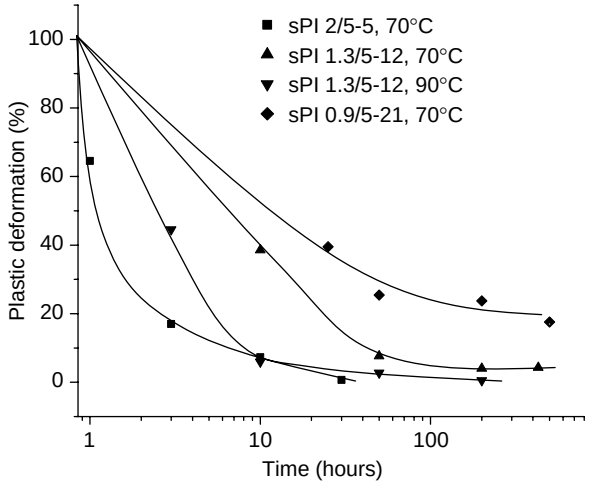

Fig. 4. Normalized plastic deformation for different sPI and temperature as a function of ageing time in water.

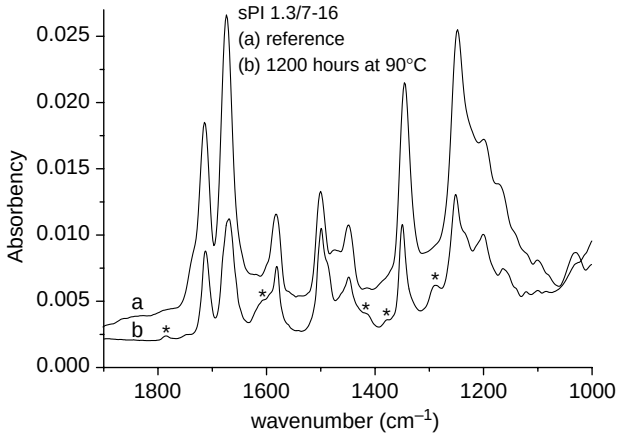

Fig. 5. FT-IR spectra of 1.3/7-16 sPI membranes: reference and aged at 90 °C during 1200 h. The different * indicated on spectrum b correspond to new absorption bands characteristic of degradation.

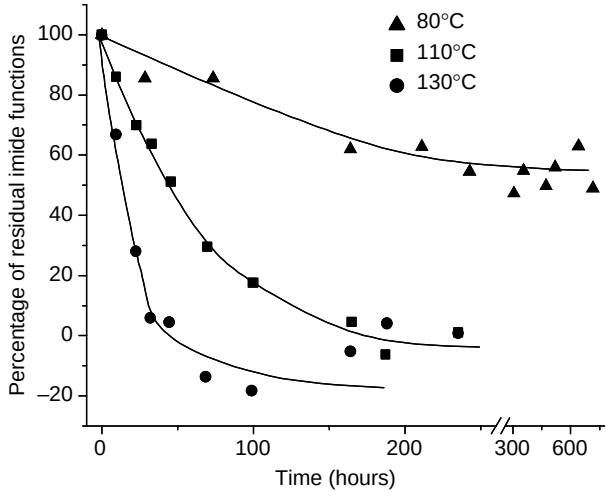

Fig. 6. Percentage of residual imide functions against ageing time in water for different temperatures ranging from 80 to 130 °C and a sPT 0.9/5–21 membrane.

It is surprising to propose the formation of anhydride groups in a water swollen membrane but the naphthalenic anhydride is a very stable structure. Indeed, it is very difficult to completely hydrolyse the naphthalenic dianhydride monomer even at high temperature and the anhydride formation has already been observed in a NMR study of sulfonated naphthalene imide model compounds [22]. These new absorption bands appear only after long ageing times compared to the loss of the mechanical properties and their intensity is always pretty low suggesting a fast elution of the degradation products. For shorter ageing times, the main effect of ageing on IR spectra is a strong decrease in intensity of some characteristic bands and especially the ones related to the imide functions (1350 cm^{-1}) confirming the proposed mechanism.

Since it can be assumed that, at the first stage of the degradation, the hydrophobic part of the polymer is not significantly altered, a specific band from the hydrophobic part can be used to normalize the spectra. The 1500 cm^{-1} band corresponding to a C=C stretching vibration in the ODA monomers was chosen for this purpose. From the intensity of the normalized 1350 cm^{-1} band, the remaining quantity of imide functions in the ionic sequence can be calculated. Two series of experiments were carried out either by attenuated total reflection (ATR) on both side of a 50 μm thick membrane or by transmission on thin films. These later experiments give an average response of membrane degradation along thickness. All the results were found to be very similar indicating that the degradation is homogeneous along the membrane thickness and that the results are not influenced by the elution rate of the degradation products. Fig. 6 presents the evolution of residual imide functions in 0.9/5-21 sPI membrane against ageing time in water for different temperatures ranging from 80 to 130 °C. At 110 and 130 °C, the imide functions in the ionic sequence are completely hydrolyzed in less than 200 h. The few negative points observed for the experiments at 130 °C suggest that the hydrophobic part of the polymer could be partially hydrolyzed at this elevated temperature. On the contrary, at 80 °C, a plateau is observed for long ageing times corresponding to 45% of the imide functions remaining in the ionic sequences. These results appear to be in good agreement with the data obtained from mechanical measurements (Fig. 3). Reproducing the same experiment at 90 °C, a plateau was also found but corresponding to only 20% of remaining imide functions. The IR results thus suggest that the hydrolysis reaction of imide function is equilibrated and that the equilibrium constant strongly depends on the temperature due to both an increase in mobility and in solubility of the degradation products. Depending on the ageing conditions, the recombination can also be hindered by consumption of some reactants by side chemical reactions. For example, the amine functions produced by hydrolysis are known to be sensitive to oxidation and this reaction is likely to be temperature dependent. From the initial slopes deduced from Fig. 6, an activation energy around 60 kJ/mol can be deduced, which corresponds to the classical values determined for polyimide hydrolysis [24,25].

The effect of block length on the hydrolysis kinetics was analyzed for two different IECs, 1.3 and 2 mequiv./g. The initial number of imide functions per ionic sequence are 6, 10 and 18 for $X=3$, 5 and 9 reference membranes. After 200 h of ageing in water at 90 °C, the numbers of residual imide functions per ionic sequences are, respectively, 4.3, 4.5 and 7.2 for the $X=3$, 5 and 9 1.3 mequiv./g sPI and 1.8, 4.7 and 13.5 for the 2 mequiv./g sPI. In both cases, the number of residual imide functions increases with the ionic block length but opposite behaviours are observed when plotted as relative percentage (Fig. 7(A) and (B)). For 2 mequiv./g sPI, the degradation is faster decreasing the block length and, surprisingly, it is faster for long ionic sequences in the case of 1.3 mequiv./g sPI membranes. The loss of imide functions can be due either to their hydrolysis or to elution of ionic oligomers consecutive to two chain scissions. The mobility of long oligomers is expected to be very low within the membrane but they are more soluble in water than short ones. Indeed, the BDSA is poorly soluble in water due to a complex formation between the terminal amine and the sulfonic acid groups while an oligomer with $X=5$ is readily soluble in water probably

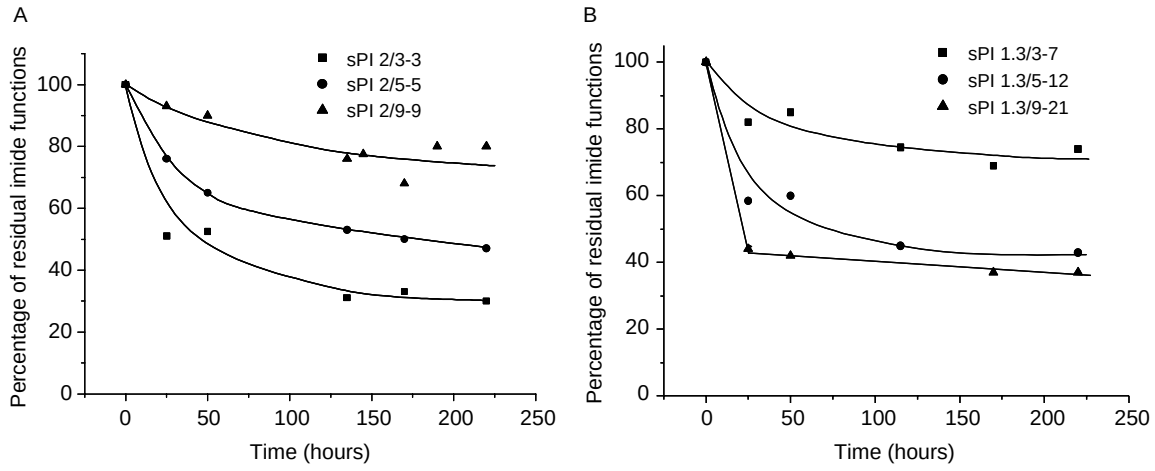

Fig. 7. Percentage of residual imide functions against ageing time in water at 90 °C depending on the block character (A) 2 mequiv./g sPI; (B) 1.3 mequiv./g sPI.

because the 10 SO_3H are not counterbalanced by the two terminal amine groups. In addition, it has been shown that increasing the block length and decreasing the IEC favours a macroscopic phase separation between ion rich and ion poor phases [26]. This phase separation is particularly visible for the 1.3/9-21 and 1.3/7-16 sPI membranes, which are no more transparent. The origin of this phase separation has not been yet clearly elucidated but it is likely to be due to the block character. With $X=9$ and IEC = 1.3 mequiv./g, the molecular weight of one repeat unit is 14,000 g/mol, which is of the same order of magnitude than the expected polymer molecular weight. Therefore, the polymer should be formed of large fractions of ABA and BAB polymers where A and B represent the ionic and hydrophobic sequences. These two components can then macroscopically phase separate in ion rich and ion poor phases due to their different solubility in *m*-cresol. In such a case, the ion rich phase presents a larger IEC close to 2 mequiv./g inducing a faster degradation rate. However, the ion poor phase should be more stable due to a lower IEC estimated to be around 0.8 mequiv./g. This hypothesis is confirmed since a plateau is observed after a fast degradation (Fig. 7(B)) indicating the occurrence of different degradation rates within each macroscopic phases while a continuous behaviour is observed for the 2 mequiv./g sPI membranes (Fig. 7(A)). In addition, freeze fractures were performed on pristine and aged membranes [26]. For the aged membrane, the fracture follows the ion rich phase indicating a complete loss of its mechanical properties while net fractures through the two phases are obtained for the pristine membrane.

The IR band at 1580 cm^{-1} attributed to naphthalene species can also be used to quantify the hydrolysis process. Its decrease in intensity can be related to the IEC value since the disappearance of naphthalene moieties is only possible by elution with the degradation products when associated with sulfonated benzidine monomers. The analysis conducted for both 1.3 and 2 mequiv./g sPI membranes in water at 90 °C reveals that the kinetics of disappearance of naphthalene moieties are identical to the loss of imide functions. This result confirms that the elution of the degradation products is a fast process compared to the hydrolysis of the imide functions, which appears as the limited phenomenon. This experiment also confirms that the hydrolysis is mainly occurring in the ionic sequences. In the case of a significant hydrolysis in the hydrophobic part of the polymer, the degradation products would not be extracted from the membrane since they are not water soluble. Therefore, the 1580 cm^{-1} band should not be affected while the total number of imide functions should significantly decrease. This is not experimentally observed.

3.3. Sulfonate content

The sulfonate content can be determined by scanning electron microscopy coupled with X-ray energy dispersive analysis (SEM-EDX). We have first verified the homogeneity of the degradation across the 40 μm thick membrane through the determination of sulfur profiles. The profiles are completely flat whatever the membrane, temperature of degradation and ageing time. The degradation effect is only an overall decrease in the sulfur quantity with an increase in statistical dispersion (Fig. 8). The sulfur profiles reveal that the membrane thickness is not modified by the ageing despite a significant loss of

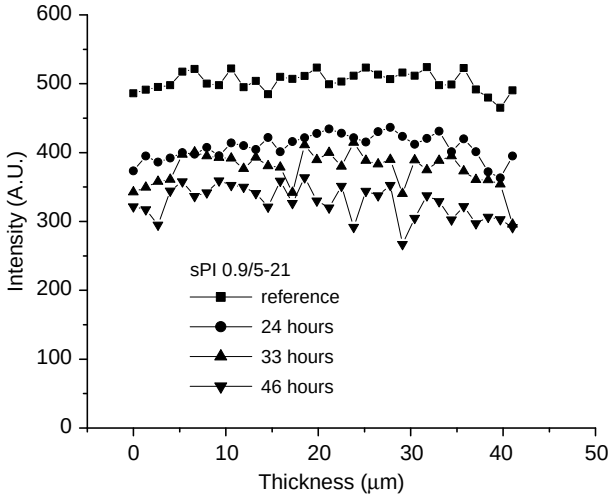

Fig. 8. Sulfur concentration profiles for 0.9/5-21 sPI depending on the ageing time.

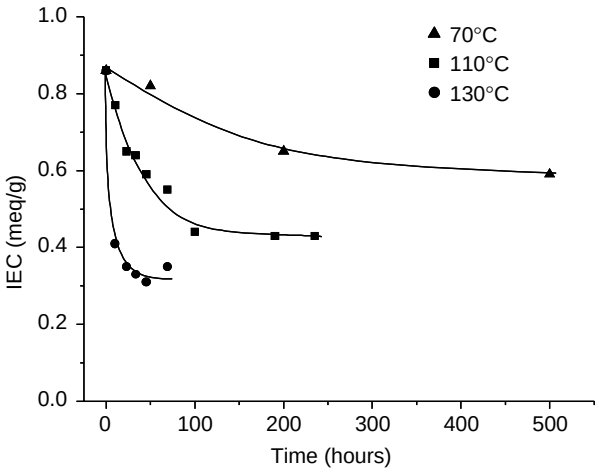

Fig. 9. IEC evolution followed by SEM EDX sulfur profile as a function of ageing time for 0.9/5-21 sPI and different temperatures.

matter. This is mainly due to the very rigid polymer structure and the very high glass transition temperature, which does not allow polymer reorganization upon ageing. Indeed, the T_g is higher than 250 °C, temperature at which the thermal decomposition begins. The EDX analysis was then integrated on larger surfaces ($10\times10\ \mu m^2$) and the IEC values were extracted thanks to a calibration curve.

Degradation kinetics were determined for various membranes and temperatures. Fig. 9 shows the IEC evolution as a function of ageing time for 0.9/5-21 sPI at three temperatures. Two different behaviors are observed depending on temperature: in the 70–90 °C range the kinetics are very similar within the experimental errors while a strong effect of temperature is observed for higher temperatures. For each curve a plateau is observed for long ageing times and its level is directly related to the ageing temperature. The infrared study indicates that most of the imide functions have disappeared from the ionic sequences due to either hydrolysis or elution of sulfonated oligomers. Therefore, a complete disappearance of the sulfonic groups could be expected. However, as previously noted, the benzidine di sulfonic acid (BDSA) monomer is poorly soluble in water due to ionic cross-links between the terminal amine functions and the sulfonic acid groups. As the oligomer length increases, there is an increasing excess of SO_3H groups with respect to amine functions that enhances the water solubility. Therefore, the quantity of remaining sulfonic acid groups within the membranes is not directly related to the number of polymer chain scissions.

3.4. Structural evolution

The membranes were analyzed by solid ^{13}C NMR using CPMAS and HPDEC NMR sequences in order to identify some structural evolution upon ageing. A 2/5-5 membrane immersed 100 h in water at 90 °C was compared to a pristine membrane. No significant difference was observed on both dry and swollen state except a decrease of the intensity of the NMR band associated to imide carbon (153 ppm). No increase in mobility is observed, which could be associated to the mobile oligomers in swollen aged membrane using the HPDEC sequence confirming that most of the oligomers are quickly eluted out from the membrane or strongly ionically cross-linked.

The SAXS–WAXS spectra of sPI membranes reveal a multi scale structure, which extends from the nanometer to the micrometer (ultra low angles). These patterns have been studied depending on the IEC, the water content, the nature of the counterions and the membrane orientation with respect to the X-ray beam [7,9,27]. The spectra which are highly anisotropic were interpreted as originating from a foliated structure packed along the membrane thickness. In the present experiments, the membranes have been studied with the X-ray beam perpendicular to the membrane plane and they have been neutralized with cesium ions in order to increase the contrast between the ionic domains and the polymer matrix. As most of ionomer membranes [28–30], the SAXS spectra exhibit a broad maximum (usually called ionomer peak) and an upturn in intensity at low angles. However, the ionomer peak is located at very low q values, which was attributed to the block character. In addition, this maximum, the intensity of which is directly related to the counterion electron density does not shift toward lower angles upon swelling. The effect of ageing, which is clearly visible on the spectra, mainly consists of a continuous disappearance of the ionomer peak as a function of ageing time (Fig. 10). Since, the ageing temperature is far below the glass transition temperature no structural reorganization is expected for these membranes. Therefore, one may attribute the decrease of the scattering peak intensity to the loss of sulfonate groups and consequently to the decrease of cesium concentration in the ionic domains, which induces a decrease of the electron density contrast with the polymer matrix.

A 2/5-5 sPI membrane was analyzed by infrared spectroscopy after a fuel cell test at 80 °C. In order to extract an average response for the chemical modifications, the aged membrane was neutralized with alkyl ammonium ions and dissolved in cresol. A thin film (5 μm) was then prepared by

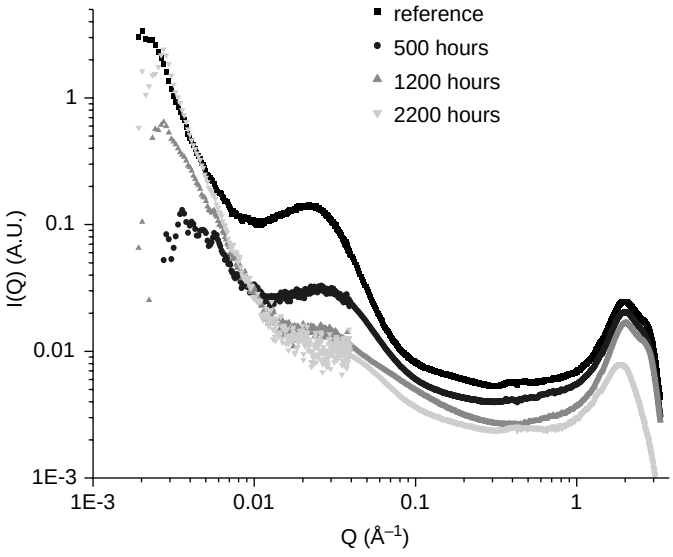

Fig. 10. SAXS spectra obtained for a Cs^+ neutralized 1.3/3-7 sPI membrane depending on the aging time in water at 90 °C.

solution casting for transmission measurements. The IR spectrum is very similar to those obtained after an ex situ ageing in pure water which suggests that the hydrolysis is the main degradation process in fuel cells. However, the quantitative analysis of the imide functions reveals that the degradation kinetic is significantly faster in fuel cell indicating either that an additional degradation mechanism occurs or that the hydrolysis process is accelerated by the electrochemical reactions. Typically, after 30 h of fuel cell operation, 55% of the imide functions have disappeared while 350 h are necessary to produce the same damage in pure water at the same temperature.

The membrane degradation in fuel cell conditions is often considered to be strongly influenced by the presence of radicals, which could be formed by electrochemical reactions. It is not clear if these radicals are produced by an incomplete oxygen reduction at the cathode or by a reaction at the anode due to oxygen permeation through the membrane. However, it is commonly accepted that these radicals are likely to be $HO^{\cdot}$ radicals, which can be mimicked ex situ by immersing the membranes in hydrogen peroxide solutions at elevated temperatures. A 2/5-5 sPI membrane was then aged 30 h at 80 °C in a 3% H_2O_2 solution. Its infrared spectra is very similar to the one obtained after aging in pure water but the degradation kinetic as revealed by the imide function absorption band is strongly accelerated. Since, the mechanical properties were completely lost within few hours, the H_2O_2 concentration was decreased to 0.5% and the degradation kinetic was followed by infrared (Fig. 11). The loss of imide function is still significantly faster than the degradation observed in fuel cell conditions. Fifty-five percent of the imide functions are lost in 4 h while the same degradation is observed after 30 h of operation in fuel cell. By interpolation between the experiments performed in pure water and in 0.5% H_2O_2, it was deduced that the H_2O_2 concentration corresponding to the fuel cell aging was roughly 0.05%. A new experiment was performed with such a concentration and the degradation observed after 30 h was similar to the one observed after the fuel cell test within the experimental uncertainties. This experiment shows that a protocol can be found to reproduce ex situ the membrane degradation in fuel cell conditions. However, it will be necessary to confirm this approach by studying the effects of the fuel cell conditions such as the cell temperature and the current density.

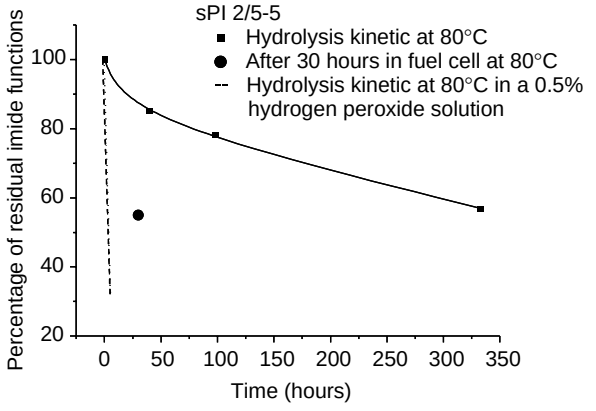

Fig. 11. Loss of imide functions as a function of ageing time in pure water (■), in a 0.5% hydrogen peroxide solution (—) and in fuel cell (●).

4. Conclusions

Series of ex situ degradation of sulfonated polyimide membranes were carried out by immersion in pure water at different temperatures. The extreme sensitivity of sPI membrane to hydrolysis was confirmed by the infrared study. This reaction was shown to be mostly complete inducing polymer chain scissions and consequently the loss of the mechanical properties. The evolution of the mechanical properties can then be used to predict qualitatively the stability of sPI in fuel cell conditions. A significant decrease of the ion exchange capacity by elution of sulfonated oligomers was revealed by both IR and SEM EDX experiments. Surprisingly, the stability depending on the ionic block length was shown to strongly depend on the ion content. For highly charged membranes, the increase of the block length stabilizes the structure while the opposite behavior is observed for lower ion content. The former result suggests that the imide functions at the interface between the neutral and ionic parts of the polymer could be more sensitive to hydrolysis. The later result is attributed to a microscopic phase separation, which increases with the ioncic sequence length. The IR analysis of a membrane after a fuel cell test reveals a faster degradation process as an effect of the presence of radicals formed by the electrochemical reaction. Hydrogen peroxide solutions appear as a representative medium to simulate degradation in fuel cell conditions. The corresponding concentration to produce the same damages on the membrane structure with the same kinetic is estimated to be around 0.05% at 80 °C.

Acknowledgements

This work has been supported by the ‘réseau PACo: membranes hautes temperatures’ (French Ministry of Research) and has been performed in the framework of the CNRS energy program (CNRS GDR 2479 Pacem, PRI CoPacem). We acknowledge Jean-François Blachot and the CERMAV for their help in the mechanical measurements, Jean-Jacques Allegraud for the numerous SEM EDX measurements, Olivier Diat and the ESRF for their help in SAXS experiments and Michel Bardet for the solid ^{13}C NMR experiments.

References

[1] Handbook of fuel cells: fundamentals, technology, applications. Wielstich W, Lamm A and Gasteiyer H (editors). Wiley; 2004.
[2] Savadogo O. J New Mater Electrochem Syst 1998;1:47–66.
[3] Rikukawa M, Sanui K. Prog Polym Sci 2000;25:1463–502.
[4] Rozière J, Jones D. Annu Rev Mater Res 2003;33:503–55.
[5] Faure S, Cornet N, Gebel G, Mercier R, Pineri M, Sillion B. Proceedings of the second international symposium on new materials for fuel cells and modern battery systems, Montréal, Canada; 1997. p. 818–27.
[6] Zhang Y, Litt M, Savinell RF, Wainrigth JS. Polym Prepr 1999;40(2): 480–1.

[7] Cornet N, Diat O, Gebel G, Jousse F, Marsacq D, Mercier R, et al. J New Mater Electrochem Syst 2000;3:33–42.
[8] Guo X, Fang J, Watari T, Tanaka K, Kita H, Okamoto K-I. Macromolecules 2002;35:6707–13.
[9] Blachot JF, Diat O, Putaux J-L, Rollet A-L, Rubatat L, Vallois C, et al. J Membr Sci 2003;214:31–42.
[10] Asano N, Miyatake K, Watanabe M. Chem Mater 2004;16:2841–3.
[11] Harris FW. Advances in materials for proton exchange membrane fuel cell systems, Asilomar, CA; 2003 [Preprint number 12].
[12] Yu J, Yi B, Xing D, Liu F, Shao Z, Fu Y, et al. Phys Chem Chem Phys 2003;5:611–5.
[13] Gode P, Ihonen J, Strandroth A, Ericson H, Lindbergh G, Paronen M, et al. Fuel Cells Fundam Syst 2003;3:21–7.
[14] Gubler L, Kuhn H, Schmidt TJ, Scherer GG, Brack HP, Simbeck K. Fuel Cells Fundam Syst 2004;4:196–207.
[15] Meyer G, Gebel G, Bardet M, Gardette J-L, Marsacq D. Fifth international symposium on new materials for electrochemical systems, Montréal; 2003. p. 256.
[16] Meyer G, Gebel G, Gonon L, Capron P, Marsacq D, Mercier R. J Power Sources; in press.
[17] Guo X, Tanaka K, Kita H, Okamoto K-I. J Polym Sci, Part A: Polym Chem 2004;42:1432–40.
[18] Miyatake K, Zhou H, Watanabe M. Macromolecules 2004;37:4956–60.
[19] Guo X, Fang J, Tanaka K, Kita H, Okada T. J Polym Sci, Part A: Polym Chem 2004;42:1432–40.
[20] Yin Y, Fang J, Watari T, Tanaka K, Kita H, Okamoto K-I. J Mater Chem 2004;14:1062–70.
[21] Genies C, Mercier R, Sillion B, Cornet N, Gebel G, Pineri M. Polymer 2001;42:359–73.
[22] Genies C, Mercier R, Sillion B, Petiaud R, Cornet N, Gebel G, et al. Polymer 2001;42:5097–105.
[23] Jamroz D, Maréchal Y. J Mol Struct 2004;693:35–48.
[24] DeIasi R, Russell J. J Appl Polym Sci 1971;15:2965–74.
[25] Heacock JF. A kinetic study of the hydrolysis of polyimide films. In: Webber WD, Gupta MR, editors. Recent advances in polyimide science and technology. Ploughkeepsie, New York: Society of Plastic Engineers; 1987. p. 174–91.
[26] Blachot JF, Diat O, Gebel G. Unpublished results.
[27] Essafi W, Gebel G, Mercier R. Macromolecules 2004;37:1431–40.
[28] Ionomers: characterization, theory and applications. Schlicu S (editor). Boca Raton: CRC Press; 1996.
[29] Ionomers: synthesis, structure, properties and applications. Tant MR, Mauritz KA and Wilkes GL (editors). London: Chapman and Hall; 1997.
[30] Gebel G, Diat O. Fuel Cells Fundam Syst 2005;5:261–76.